Microwave Review
December 2024, Vol. 30, No. 2, pp. 41-46
DOI: 10.18485/mtts_mr.2024.30.2.5

# Design and Analysis of a Defected Ground Structure T-Shaped Patch Antenna for IMT, WLAN, 5G, and 6G Applications

Yamiko Daniel Banda, Anupam Kumar Yadav, Manish Kumar, Sandeep Kumar Singh

*Abstract* – **The article presents a compact penta-band antenna designed using an FR-4 substrate, incorporating stacked T-shaped radiating elements. This antenna is tailored for use in International Mobile Telecommunication (IMT), Wireless Local Area Networks (WLAN), as well as 5th and 6th Generation (5G and 6G) mobile networks. It has compact dimensions of 57.05 × 57.43 × 1.6 mm³ and features a defective ground structure with a microstrip feedline of 3.00 mm width with an impedance of 50 Ω. The antenna operates at several key frequencies, including 2.30 GHz for IMT, 4.68 GHz for 5G (n79 band), 5.86 GHz for WLAN (IEEE 802a), 6.71 GHz, and 8.32 GHz for 6G mid-band. The 6G mid-band operation requires a bandwidth exceeding 160 MHz, covering frequencies from 7.0 to 20 GHz. Additionally, parametric studies have been carried out on the design to ensure optimal multiband performance. This makes the antenna suitable not only for current broadband systems but also for future technologies that require high efficiency and multiband capabilities.**

*Keywords* – **5G, 6G, Defected ground structure, FR-4 substrate, IMT, Penta-band, T-shaped, WLAN**

## I. INTRODUCTION

With the development of standards for wireless communication technologies, from 4th Generation (4G) to 5G and 6G, multi-band antenna design has become increasingly important. Next-generation mobile and wireless devices must operate efficiently across multiple frequency bands to support a wide range of services and applications. A compact, modified ring-shaped slot antenna with triple-band capability has enabled a single component to cover both existing and new wireless networks, making it ideal for integration into space-constrained portable devices while ensuring optimal performance across three different frequency bands [1,2]. A dual-band, low-profile monopole antenna with a double T-shaped design and stacked elements of varying sizes is also presented as a reference. This design creates separate resonance modes for the 2.4 GHz and 5.2 GHz bands, suitable for WLAN applications. Parametric studies and design modifications were conducted to achieve optimal monopole dimensions and ground plane size for maximum impedance matching [3]. Some research has focused on transforming antennas from dual-band to multi-band capabilities [3,4]. To meet the growing demands of wireless technology, researchers are exploring various techniques, including square slot antennas with L-strips [5], resonant mode coupling and excitation [6], and stub-loaded monopoles with paper clip structures [7].

Additionally, compact antenna solutions that integrate various elements are being explored for tri-band WLAN and 5G systems [8]. This highlights the trend in antenna design toward supporting multiple frequency bands simultaneously to better meet the evolving demands of wireless technology. This paper discusses a multi-band, single-fed slot antenna monopole designed for sub-6 GHz 5G applications. The antenna features a rectangular radiating slot with an inverted stub on its upper edge, which is simultaneously excited by a microstrip feed line incorporating a double-folded T-shaped structure [9]. For sub-6 GHz 5G applications, microstrip feed lines have been studied for single-fed slot antennas. In 4G, 5G, and WLAN, additional research has focused on Deca-band coverage using printed antennas, which combine C-shaped monopoles with coupling strips to cover frequencies ranging from 0.7 to 3.6 GHz, while maintaining consistent gain and efficiency [10].

This paper also provides a survey of the 3rd Generation Partnership Project (3GPP) standards for enhanced Mobile Broadband (eMBB), Ultra-Reliable Low Latency Communications (URLLC), and massive Machine Type Communications (mMTC) use cases in sub-6 GHz and mm-wave bands for 5G NR. It examines key enablers such as scalable numerology, spectrum flexibility, and lean design, along with a proposed architecture for the transition beyond 5G/6G networks [11]. The evolution of antennas from 1G to 5G has been analyzed, with a comparative study of performance indicators and various 5G antenna designs also examined in the overview [12]. To accommodate current and future wireless frequencies, redesigned printed monopole antennas were explored to achieve multi-band resonances [13-15]. In the field of 6G wireless communication, a compact portable patch antenna has been proposed by [15-17] for terahertz (THz) applications. This design uses an asymmetric coplanar waveguide (CPW) feed with curved slits on a rectangular gold-plated microstrip patch antenna to resonate at THz frequencies. Additionally, an ultra-wideband microstrip patch antenna with a defective ground surface has been introduced in [18-20].

The design includes three parasitic elements: two metallic slots shaped like an "H" and one truncated corner. The corner truncation is intended to generate resonant frequencies while also creating circular polarization (CP) [21]. In [22], a monopole antenna with a circular patch pattern is presented,

*Article history: Received April 08, 2024; Accepted September 13, 2024*

Yamiko Daniel Banda, Anupam Kumar Yadav, Manish Kumar, and Sandeep Kumar Singh are with the Department of EECE, SUSET, Sharda University, Greater Noida, 201310, India,
Emails: yamiebanda98@gmail.com,
anupamyadav11may@gmail.com, mk1038@gmail.com,
sandeepsingh.ec@sharda.ac.in

fed by a CPW with a modified internal ground plane. In [23], the antenna features three semicircular arcs positioned on the right, left, and back of the patch relative to the feed line. To enhance antenna performance, the authors adopted a new design and reduced the size of the structure. However, challenges remain in improving peak realized gain, radiation efficiency, cross-polarization levels, and the impedance bandwidth of the multiband antenna.

The proposed antenna had a T-slot introduced in the ground plane, whereas the rectangular patch has a Pi-slot, designed on an FR-4 substrate and supplied using a 50-ohm microstrip feedline. Adjusting the antenna shape achieves five different resonance frequencies, allowing for a broad working range from 2.28 GHz to 8.75 GHz that covers fundamental bands for IMT, WLAN, 5G, and the future 6G wireless systems. In addition, parametric studies have been carried out to understand the implications of crucial antenna characteristics on multi-band performance, offering design direction. The paper will be given in four sections. Section 2 discusses the antenna design technique, section 3 presents a parametric investigation, and section 4 presents the results and discussions.

TABLE 1
COMPARISON WITH OTHER PUBLISHED WORK

| [Ref] | Antenna Type | Frequency bands | Feeding Technique | Application | Antenna Size (W×L) $mm^2$ |
|---|---|---|---|---|---|
| [3] | Printed Monopole | Dual-band | Microstrip Feedline | WLAN | 75 × 75 |
| [6] | Microstrip Patch Antenna | Wideband | Microstrip Feedline | Industrial, scientific, and medica band (ISM) | 40 × 40 |
| [8] | Monopole Impedance Converter | Triple-band | Microstrip Feedline | WLAN, 5G | 120 × 60 |
| [18] | Patch Antenna with T-Slot DGS | Ultra-wideband | Microstrip Feedline | UWB Application | 70 × 50 |
| [20] | Circularly Polarised Printed Antenna | Dual-band | Coaxial Feed | WiMax, LTE | 68 × 68 |
| [21] | MIMO Antenna | Ultra-wideband | CPW-fed | UWB, WPAN, WLAN, WiMAX,5G | 64 × 70 |
| [22] | Multi-band Printed Antenna | Multi-band | Microstrip Feedline | WLAN, WiMax, LTE | 52 × 61 |
| Proposed Antenna | Microstrip Patch Antenna | Pentaband | Microstrip Feedline | IMT, WLAN, 5G and 6G | 57 × 57 |

## II. PROPOSED ANTENNA DESIGN

The baseline antenna is a compact T-shape monopole antenna with a partial ground plane and a dielectric substrate. It works in the 2.4 and 5.2 GHz WLAN spectrums, fed via a 50Ω microstrip line for impedance matching illustrated in Fig. 1(a). The T-shape and overlapped design enable the antenna to maintain a compact size compared to a standard straight monopole. The antenna resonates in two frequency bands that may be modified by varying the substrate characteristics, with the lower band less impacted than the upper band. Developing on this baseline with a tapered T-shape illustrated in Fig. 1(c) that expands the operating bandwidth, parasitic patch elements are placed on both ends of the tapered shape to produce extra resonant frequencies while achieving multi-band performances at 3.47 GHz, 5.30 GHz, and 5.68 GHz. Fig. 1(d) shows the final design with a square ring with width = 7.11 mm and 27.21 mm from the feedline width. 14 mm from the bottom of the antenna, it has a 43.01 mm length to the top. Inside the square ring, it has a rectangular shape with a 28.82 mm × 43.21 mm dimension.

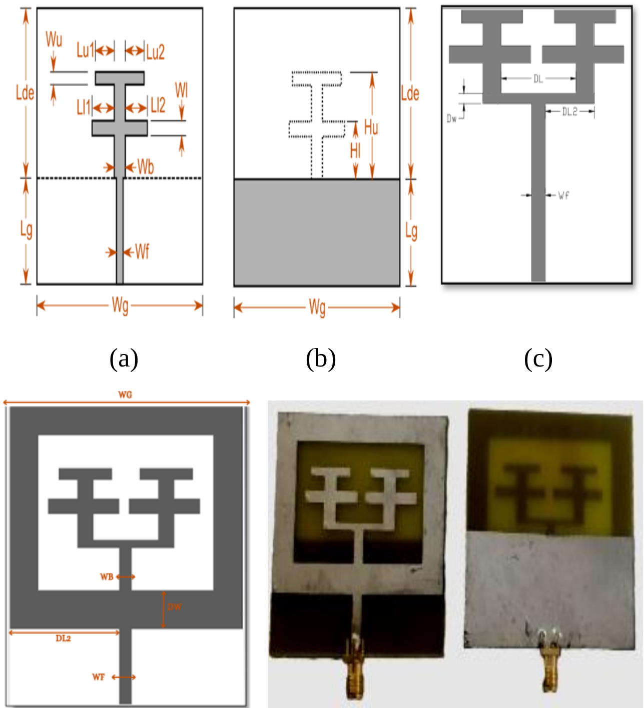


Fig. 1. The schematic of antenna design steps: (a) T-shaped design, (b) Ground plane, (c) Double T-shaped design, (d) Double T-shaped design with squared ring, (e) Fabricated antenna (Front view and Back view)

TABLE 2
STRUCTURAL DESIGN PARAMETERS LIST

| Parameter | Unit (mm) | Parameter | Unit (mm) |
|---|---|---|---|
| Copper thickness | 0.035 | *WI* | 2.73 |
| *Wg* | 54.82 | *Lu*2 | 4.63 |
| *Lg* | 27.86 | *Lu*1 | 4.61 |
| *Wf* | 2.92 | *Ll* | 6.35 |
| *Lde* | 24.23 | *Ll*2 | 7.22 |
| *Hu* | 13.08 | *DL* | 16.09 |
| *Hi* | 7.49 | *DL*2 | 10.54 |
| *Wb* | 3.90 | *Dw* | 1.6 |
| *Wu* | 2.03 | | |

## III. Parametric Study and Design Steps

A parametric study is important for achieving optimal impedance matching of the antenna. Moreover, resonating frequencies and impedance bandwidth have been effectively controlled by changing the shape and dimension of three antennas, as illustrated in Figure 1(a-d). The dimensions of the radiating elements and substrate material thickness play essential roles in antenna design, influencing the number of resonant frequencies and the antenna impedance bandwidth.

### *A. The Design Step-1 (T-Shape Antenna)*

The Figure 2. shows the first design of the antenna with dimensions of 75 × 75 × 1.6 $mm^3$ observed and the feedline width of 3 mm which is the achieved result at dual-band 2.4 GHz, and 5.8 GHz for WLAN operations.

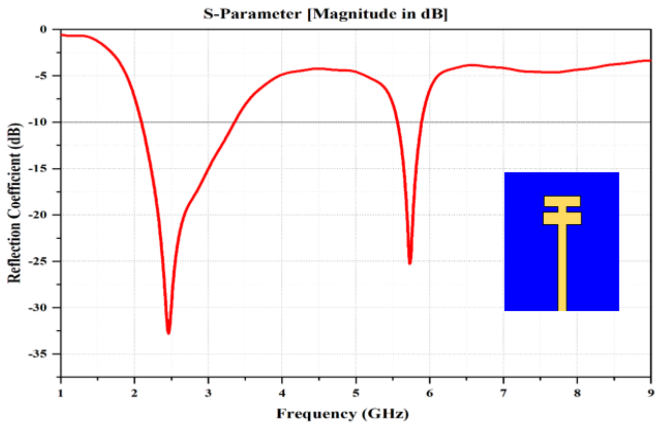


Fig. 2. |*S*11| parameters of step-1 design at 2.4 GHz, and 5.8 GHz

### *B. The Design Step-2 (T-Shape Antenna)*

The Fig. 3. Displays the second design of the antenna with dimensions of 60 × 60 × 1.6 $mm^3$ observed and the feedline width of 2.9,0 mm which the result achieved a dual-band 3.47, 5.30, and 5.68GHz, for WiMAX and WLAN operations.

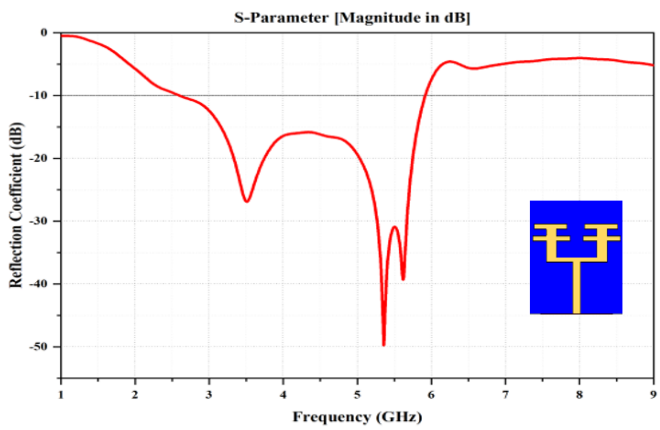


Fig. 3. |*S*11| parameters of step-2 design at 3.47, 5.30, and 5.68 GHz

### *C. The Design Step-3 (Squared Double T-Shape Antenna)*

Figure 4. displays the third step design of the proposed pentaband antenna with dimensions of 57.05 × 57.43 × 1.6 mm3 observed and the feedline width of 3 mm, which is the achieved result for IMT, WLAN, 5G, and 6G applications.

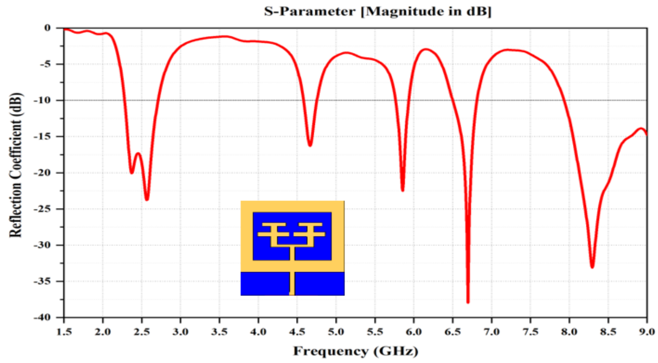


Fig. 4. |*S*11| parameters of step-3 design at 2.30 GHz, 4.68 GHz, 5.86 GHz, 6.71 GHz, and 8.32 GHz.

## IV. Simulated Results

### *A. $|S_{11}|$ Parameter*

The graphical representation of the data pair helps optimize key details such as impedance matching and beam width. Understanding an antenna’s radiation properties and performance is critical for ensuring strong signal transmission, particularly when designing and integrating directional antennas. Both the E-plane and H-plane patterns must be considered. This design functions effectively across five different frequency bands: 2.30 GHz, 4.68 GHz, 5.86 GHz, 6.71 GHz, and 8.32 GHz, as shown in Figures 6 (a-e) and 7 (a-e).

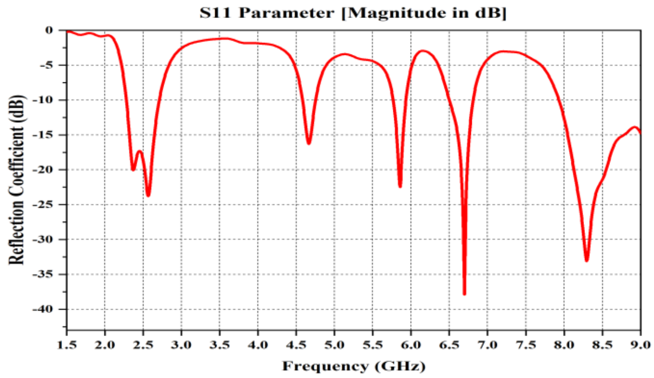


Fig. 5. Optimal |S11| parameters of the proposed penta-band antenna at 2.30 GHz, 4.68 GHz, 5.86 GHz, 6.71 GHz, and 8.32 GHz

### *B. Radiation Pattern*

The graphical representation of the data pair helps optimize key details such as impedance matching and beam width. Understanding an antenna's radiation properties and performance is critical for ensuring strong signal transmission, particularly when designing and integrating directional antennas. Both the E-plane and H-plane patterns must be considered. This design functions effectively across five different frequency bands: 2.30 GHz, 4.68 GHz, 5.86 GHz, 6.71 GHz, and 8.32 GHz, as shown in Figures 6 (a-e).

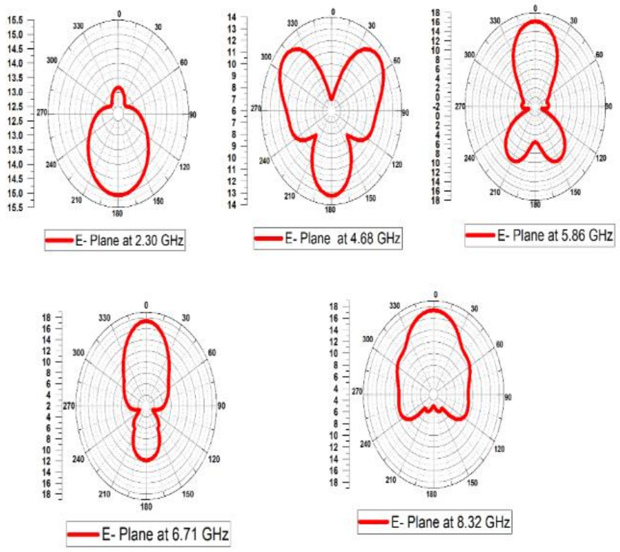


Fig. 6. E-plane pattern of the proposed pentaband antenna at: (a) 2.30 GHz, (b) 4.68 GHz, (c) 5.86 GHz, (d) 6.71 GHz, (e) 8.32 GHz

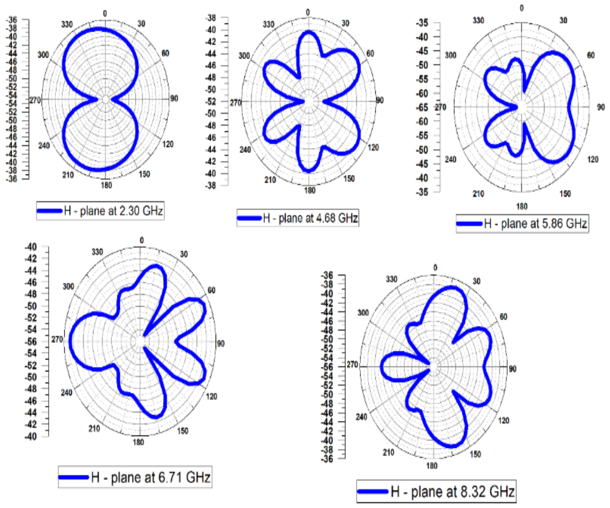


Fig. 7. H-plane pattern of the proposed pentaband antenna at: (a) 2.30 GHz, (b) 4.68 GHz, (c) 5.86 GHz, (d) 6.71 GHz, (e) 8.32 GHz

*C. Surface Current Density*

The surface current density indicates the amount of electric current focused on the antenna's conducting surface. In this research, the simulated distributions at the three frequencies (2.30 GHz, 4.68 GHz, 5.86 GHz, 6.71 GHz, and 8.32 GHz) demonstrate differences in the observed radiation pattern features. This significant margin concentration and lack in the center corresponds to the highly concentrated main beam typically generated on the patch surface. The changing current density as a function of frequency correlates directly to the multi-band microstrip antenna's radiation pattern performance, developing the different directed patterns required at the tuned operating bands, as illustrated in Fig. 8 (a-e).

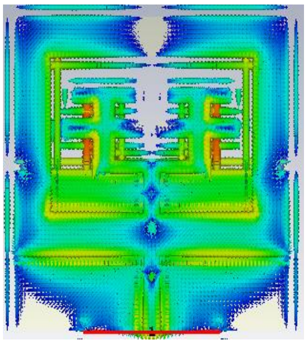

(a)

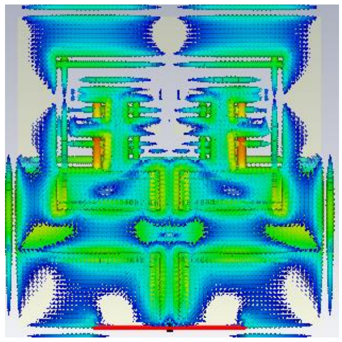

(b)

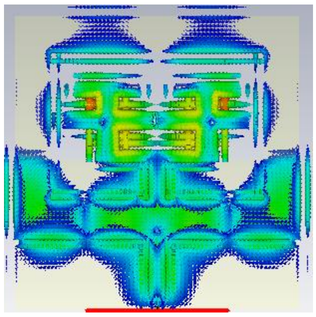

(c)

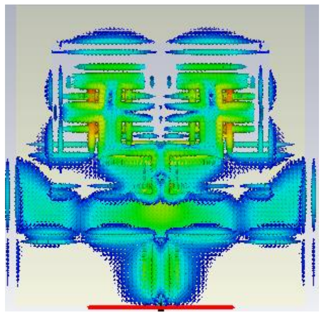

(d)

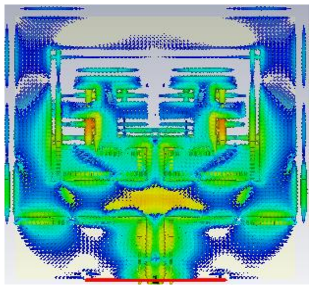

(e)

Fig. 8. Surface current density proposed Pentaband antenna at: (a) 2.30 GHz, (b) 4.68 GHz, (c) 5.86 GHz, (d) 6.71 GHz, (e) 8.32 GHz

*D. Directivity*

The antenna has desired characteristics in a variety of applications, allowing it to focus its energy in a specific direction. At 2.30 GHz, the directivity increases as it moves from lower frequencies to higher frequencies, with 3.99 dBi and relatively low radiating energy in various directions at this frequency. At 4.68 GHz, the directivity is 4.46 dBi; at 5.86 GHz, it is 5.70 dBi; at 6.71 GHz, it is around 7.97 dBi; and at 8.31 GHz, it is 7.06 dBi higher than the lower frequency. The antenna becomes more effective at concentrating its energy in a particular direction, especially at the frequency 6.71 GHz, where it achieves its directivity while proving both efficient power transfer and increasing directionality at higher frequencies, making it suitable for applications demanding focused signal transmission within the designated spectrum, as illustrated in Fig. 9.

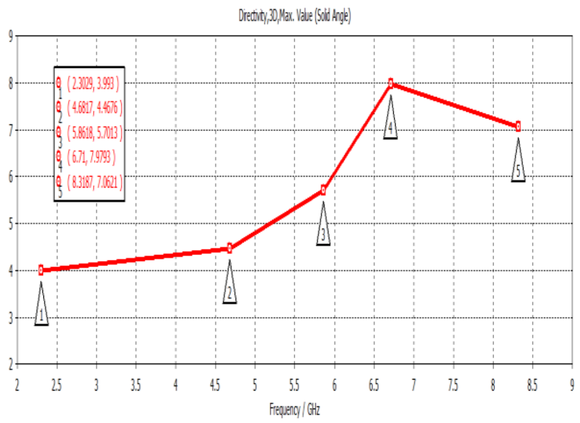


Fig. 9. Directivity of the proposed pentaband antenna at 2.30 GHz, 4.68 GHz, 5.86 GHz, 6.71 GHz, and 8.32 GHz

## V. Measured Results

The experimental verification of the proposed pentaband antenna on a Rohde & Schwarz ZNB 8 Vector Network Analyzer, load, and cable aims to examine and confirm the findings obtained through simulation or mathematical computations of antenna prototypes built and modified to achieve acceptable performance based on the simulation results.

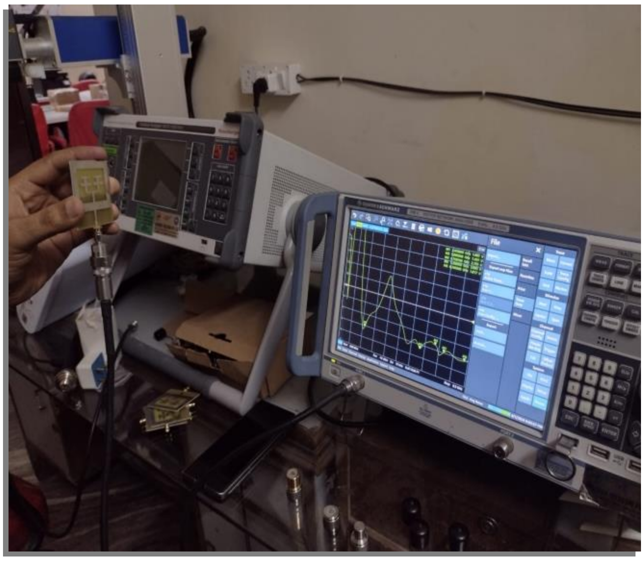

Fig.10. Experimental validation of proposed pentaband antenna

### A. Voltage Standing Wave Ratio

A VSWR of less than 2 indicates that the antenna is efficiently transmitting and receiving signals with minimal reflection losses. This value is well within the acceptable range, which is typically considered to be below 2.0 for most communication systems. The results validate the proper functioning of the antenna and its suitability for deployment in our intended applications.

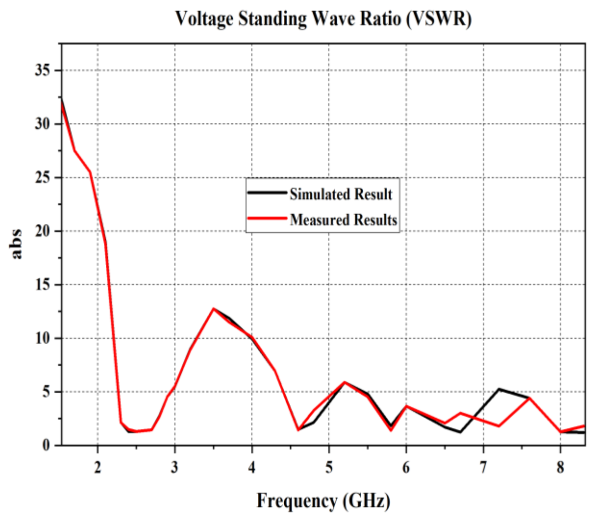


Fig. 11. VSWR parameters of the proposed penta-band antenna at 2.30 GHz, 4.68 GHz, 5.86 GHz, 6.71 GHz, and 8.32 GHz

### B. Gain

The gain measurements demonstrate that the gain increases with frequency. The five frequencies represent the antenna emitting power in a specific direction at these frequencies. The measurements show the amount of power transmitted in specific directions that can be radiated when isotropic radiation occurs. However, the gain also depends on the antenna size, geometry, and efficiency. The gain values at these frequencies are vital for evaluating the antenna performance in various wireless applications, including IMT, WLAN, 5G, and 6G networks, as illustrated in Fig. 12.

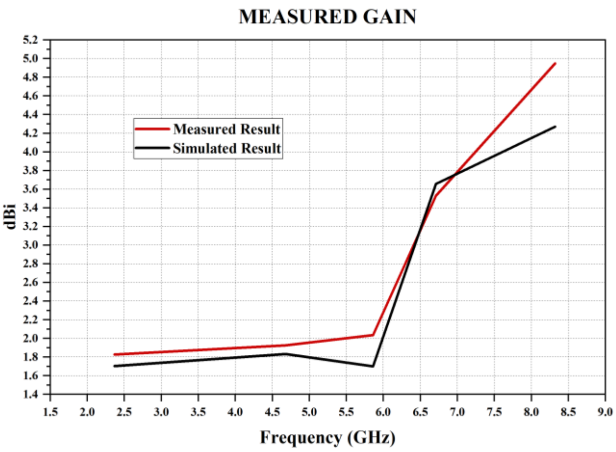


Fig. 12. Gain of the proposed pentaband antenna at 2.30 GHz, 4.68 GHz, 5.86 GHz, 6.71 GHz, and 8.32 GHz.

## VI. Conclusion

The design and optimization of a novel multi-band antenna operating at 2.30 GHz, 4.68 GHZ, 5.86 GHz, 6.71 GHz, and 8.32 GHz allows the compact planar antenna to provide reliable high-speed wireless connectivity for a diverse range of modern applications and standards, including IMT, WLAN according to 802.11 specifications, 5G NR, IoT devices, and 6G wireless communication. An antenna is tailored to achieve optimal radiation characteristics, impedance matching, interference mitigation, and data rates to overcome the challenges of mobility, throughput, co-existence, and form factor in modern hyper-connected wireless devices that demand seamless performance across multiple bands, standards, and use cases. The simulated results validated the designed antenna as a suitable option for IMT, WLAN, 5G, and 6G wireless communication applications.

## REFERENCES


[1] C. A. Balanis, *Antenna Theory,* John Wiley & Sons, 2012.

[2] S. P. Gangwar, K. Gangwar, and A. Kumar, “A Modified Ring-Shaped Slot Radiator for Triple-Band Wireless Applications”, *Microwave Review*. vol. 26., no. 1, pp.15-21, 2020.

[3] Y. L. Kuo and K. L. Wong, “Printed Double-T Monopole Antenna for 2.4/5.2 GHz Dual-Band WLAN Operations”, *IEEE Trans Antennas Propag*, vol. 51, no. 9, pp. 2187–2192, 2003, DOI: 10.1109/tap.2003.816391.

[4] M. A. Chung and C.W. Yang, “A Miniaturized Planar Monopole Antenna Based on a Coupling Structure for Compact Mobile Internet of Things and Electric Vehicles Device Applications in 5G, LTE, WLAN, WiMAX, Sirius/XM Radio, V2X, and DSRC Wireless Systems”, *Int J Antennas Propag*, vol. 2021, pp. 7535382, 2021, DOI: 10.1155/2021/7535382

[5] W. Hu, Y. Z. Yin, P. Fei, and X. Yang, “Compact Triband Square-Slot Antenna with Symmetrical L-Strips for WLAN/WiMAX Applications”, *IEEE Antennas Wirel Propag Lett*, vol. 10, pp. 462–465, 2011, DOI: 10.1109/lawp.2011.2154372.

[6] M. Hussein, H. Alrudainy, W. Abdulkawi, A. Alieldin, and S. Alshamrani, “A Low-Profile Wideband Microstrip Patch Antenna with Simple Configuration”, *Microwave Review*, vol. 29, no. 2, pp. 3–6, 2023, DOI:10.18485/mtts_mr.2023.29.2.1.

[7] H. Zhai, L. Liu, Z. Ma, and C. Liang, “A Printed Monopole Antenna for Triple-Band WLAN/WiMAX Applications”, *Int J Antennas Propag*, vol. 2015, pp. 1–7, 2015, DOI: 10.1155/2015/254268.

[8] H. Zhuang, “A Triple-Band Microstrip Antenna with a Monopole Impedance Converter for WLAN and 5G Applications”, *Int J Antennas Propag*, vol. 2022, pp. 1–9, 2022, DOI: 10.1155/2022/3339240.

[9] I. Ishteyaq, I. Shah Masoodi, and K. Muzaffar, “A Compact Double-Band Planar Printed Slot Antenna for Sub-6 GHz 5G Wireless Applications”, *Int J Microw Wirel Technol*, vol. 13, no. 5, pp. 469–477, 2020, DOI: 10.1017/s1759078720001269.

[10] M. Yang, Y. Sun, and F. Li, “A Compact Wideband Printed Antenna for 4G/5G/WLAN Wireless Applications”, *Int J Antennas Propag,* vol. 2019, pp. 3209840, 2019, DOI: 10.1155/2019/3209840.

[11] A. Dogra, R. K. Jha, and S. Jain, “A Survey on beyond 5G Network with The Advent of 6G: Architecture and Emerging Technologies”, *IEEE Access*, vol. 9, no. 2169–3536, pp. 1, 2020, DOI: 10.1109/access.2020.3031234.

[12] A. P. Reddy, P. Muthusamy, "Enhancement of Bandwidth and Gain using Proximity Coupled DGS Structure Patch Antenna for WiMAX/5G Band Applications”, *Microwave Review,* vol. 28, pp. 23, 2022.

[13] P. B. Nikam, J. Kumar, A. Baidya, and A. Ghosh, “Low-Profile Bandwidth and E-plane Radiation Pattern Reconfigurable Patch Antenna for Sub-6 GHz 5G Applications”, *AEU - International Journal of Electronics and Communications*, vol. 157, pp. 154415, 2022, DOI: 10.1016/j.aeue.2022.154415.

[14] I. Ahmad, W. Tan, Q. Ali, and H. Sun, “Latest Performance Improvement Strategies and Techniques Used in 5G Antenna Designing Technology, a Comprehensive Study”, *Micromachines (Basel),* vol. 13, no. 5, pp. 717, 2022, DOI: 10.3390/mi13050717.

[15] K. K. Naik, “Asymmetric CPW-fed Patch Antenna with Slits at Terahertz Applications for 6G Wireless Communications”, *Wireless Networks*, vol. 30, pp. 2343–2351, 2024, DOI: 10.1007/s11276-024-03695-4.

[16] H. Vettikalladi, W. T. Sethi, and W. Ko, “Sub-Terahertz (THz) Antenna for Internet of Things and 6G Communication”, *Frequenz*, vol. 76, no. 3–4, pp. 177–184, 2021, DOI: 10.1515/freq-2021-0074.

[17] T. O. Olawoye and P. Kumar, “A High Gain Antenna with DGS for Sub-6 GHz 5G Communications”, *Advanced Electromagnetics*, vol. 11, no. 1, pp. 41–50, 2022, DOI: 10.7716/aem.v11i1.1670.

[18] S. Jabeen and G. Hemalatha, “Microstrip Fed Pi-Slot Patch Antenna with T-Slot Dgs for UWB Applications”, *Progress In Electromagnetics Research C*, vol. 129, pp. 63–72, 2023, DOI: 10.2528/pierc22112804.

[19] M. E. Yassin, H. A. Mohamed, E. A. F. Abdallah, and H. S. El-Hennawy, "Single-Fed 4G/5G Multi-Band 2.4/5.5/28 GHz Antenna*”, IET Microwaves, Antennas & Propagation*, vol. 13, no. 3, pp. 286–290, 2019, DOI: 10.1049/iet-map.2018.5122.

[20] P. Kiran, R. Mownika, D. Ajay, N. Nagesh and Singh, Vivek. “Compact Ultra-Wideband Multilayer Patch Antenna with Defected Ground Plane for Ku Band Applications”, *Microwave Review*, vol. 29, no. 1, pp. 16-23, 2023.

[21] A. K. Nayak, P. K. Subudhi, S. B. Panda and R. K. Nanda, "Dual-Band Circular Polarized Printed Antenna for WiMAX and LTE Applications”, *IEEE International Symposium on Smart Electronic Systems*, Rourkela, India, 2019, pp. 340-343, DOI: 10.1109/iSES47678.2019.00085

[22] P. Rakluea *et al.*, “Flexible Thin Film-Based Triple Port UWB MIMO Antenna with Modified Ground Plane for UWB, WLAN, WiMAX, WPAN and 5G Applications”, *IEEE Access*, vol. 11, pp. 107031–107048, 2023, DOI: 10.1109/access.2023.3320181.

[23] P. K. Mishra, A. K. Nayak and K. C. Rout, "Design and Testing of a Multi-Band Printed Antenna for WLAN/WiMAX/LTE Applications”, *IEEE International Symposium on Smart Electronic Systems*, Rourkela, India, 2019, pp. 201-204, DOI: 10.1109/iSES47678.2019.00052